Electronic Supplementary Material (ESI) for Journal of Materials Chemistry C.

Supporting Information

Tune the Aggregation-induced Emission Behavior of Novel Luminescence Probes for DNP and Fe^{3+} Sensing by Molecular Packing

Yaru Song[+a], Jie Dong[+b], Jiangyan Yuan[a], Xinyu Zhang[a], Guoling Wu[a], Enbing Zhang[a], Guangyuan Feng[a], Lingli Wu[c,*], Shengbin Lei[a,*] and Wenping Hu[a]

[a] *Tianjin Key Laboratory of Molecular Optoelectronic Sciences, Department of Chemistry, School of Science & Collaborative Innovation Center of Chemical Science and Engineering, Tianjin University*
Tianjin, Tianjin 300072 (China)
E-mail: shengbin.lei@tju.edu.cn
[b] *School of Chemistry and Chemical Engineering, Henan University of Technology*
Zhengzhou, Henan 450001 (China)
[c] *Medical College, Northwest Minzu University*
Lanzhou, Gansu 730000 (China)
E-mail: wulingli19831106@163.com
[+] *These authors contributed equally to this work*

Table of Contents

1. Experimental Section

Carbazole (99 %), benzyltriethylammonium chloride (BTEAC, 98%), 2,5-dihydroxyterephthalaldehyde (97%), hydroquinone (98%), 2,5-di-tert-butylbenzene-1,4-diol (98%), 2,5-dibromobenzene-1,4-diol (98%) were purchased from Tianjin Chinese Ciensi Technology Co., Ltd. Benzene (AR) and various explosive analogues for sensing were purchased from Shanghai Chinese Aladdin Technology Co., Ltd. Sodium hydroxide (AR), potassium carbonate (K_2CO_3, AR) and various metal ion salts for sensing were purchased from Tianjin Chinese Jiangtian Chemical Technology Co., Ltd. The synthetic route of a series of novel biscarbazole-type molecules is shown in Figure S1.

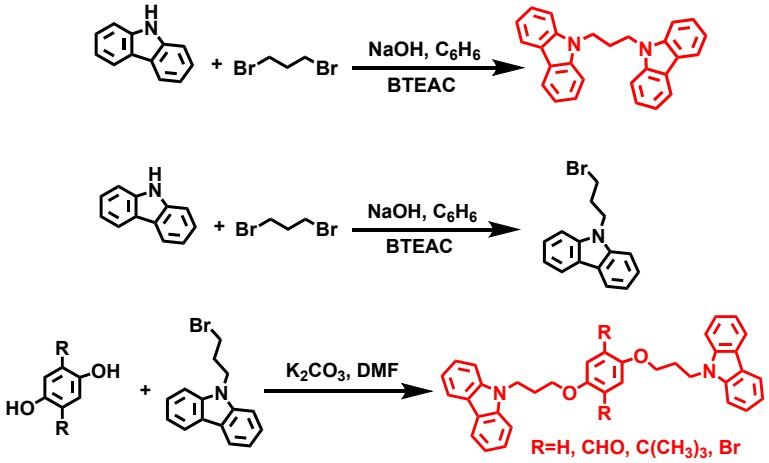

Figure S1. Synthetic route for a series of biscarbazole organic small molecules (TPAK, DCP, BCP, TBCP and BBCP).

1.1 Synthesis of 2,5-bis(3-(9H-carbazol-9-yl)propoxy)terephthalaldehyde (TPAK):

9-(3-bromopropyl)-9H-carbazole was synthesized acodding to our previous work (Reference 1). 2,5-bis(3-(9H-carbazol-9-yl)propoxy)terephthalaldehyde (TPAK) was synthesized as follow: In a round bottom flask, 2,5-dihydroxyterephthalaldehyde (250 mg, 1.5 mmol) was dissolved in 7 ml of DMF, then 9-(3-bromopropyl)-9H-carbazole (1.96 g, 6.8 mmol) and potassium carbonate (843.6 mg, 6.1 mmol) were added. And the reaction mixture was stirred under argon at 40 ℃ overnight. And then extracted with ethyl acetate (3×60 mL). The organic layer was dried over anhydrous Na_2SO_4. After removal of the solvent, the residue was purified by column chromatography on silica gel with petroleum ether-dichloromethane (3:1) as eluent to afford the product as a yellow powder (562 mg, 64%). ^{1}H NMR (400 MHz, $CDCl_3$) δ 10.41 (s, 2H), 8.10 (d, J = 7.7 Hz, 4H), 7.39 (t, J = 8.9 Hz, 8H), 7.28 (s, 2H), 7.23 (t, J = 7.2 Hz, 4H), 4.57 (t, J = 6.4 Hz, 4H), 4.09 (t, J = 5.3 Hz, 4H), 2.44 (s, 4H). ^{13}C NMR (101 MHz, $CDCl_3$) δ 188.52, 154.67, 140.25, 129.01, 125.82, 122.98, 120.56, 119.16, 111.78, 108.31, 66.19, 39.60, 28.48. HRMS calcd for: $C_{38}H_{32}N_2O_4^+$ $[M+Na]^+$: 603.2254, found: 603.2256.

1.2 Synthesis of 1,3-di(9H-carbazol-9-yl)propane (DCP):

To a mixture of carbazole (5.0 g, 30 mmol), benzene (15 ml), benzyltriethylammonium chloride (BTEAC) (250 mg), and aqueous (50%) sodium hydroxide solution (15 ml), an excess amount (more than 10 times equivalent to carbazole) of alkyl dibromide was added with stirring. And then extracted with dichloromethane (3×50 mL). The organic layer was dried over anhydrous Na_2SO_4. After removal of the solvent, the residue was purified by column chromatography on silica gel with petroleum ether-dichloromethane (10:1) as eluent to afford the product as a white gray powder (1.96 g, 35%). ^{1}H NMR (400 MHz, $CDCl_3$) δ 8.11 (d, J = 7.7 Hz, 4H), 7.41 (d, J = 8.2 Hz, 4H), 7.25 – 7.18 (m, 8H), 4.37 (t, J = 7.3 Hz, 4H), 2.56 – 2.41 (m, 2H). ^{13}C NMR (101 MHz, $CDCl_3$) δ 140.09, 125.81, 123.05, 123.01, 120.55, 119.12, 108.43, 77.35, 77.03, 76.71, 56.07, 40.73, 32.48. HRMS calcd for: $C_{27}H_{22}N_2^+$ $[M]^+$: 374.1783, found: 374.1785.

1.3 Synthesis of 1,4-bis(3-(9H-carbazol-9-yl)propoxy)benzene (BCP):

In a round bottom flask, hydroquinone (55 mg, 0.5 mmol) was dissolved in 6 ml of DMF, then 9-(3-bromopropyl)-9H-carbazole (0.67 g, 2.3 mmol) and potassium carbonate (281.2 mg, 2.0 mmol) were added. And the reaction mixture was stirred under argon at 40 ℃ overnight. And then extracted with ethyl acetate (3×60 mL). The organic layer was dried over anhydrous Na_2SO_4. After removal of the solvent, The residue was purified on large silica gel plates with petroleum ether-dichloromethane (5:1) as eluent to afford the product as a white powder (30 mg, 22%). ^{1}H NMR (400 MHz, $CDCl_3$) δ 8.10 (d, J = 6.9 Hz, 4H), 7.45 – 7.39 (m, 8H), 7.22 (ddd, J = 7.9, 6.9, 1.2 Hz, 4H), 6.79 (s, 4H), 4.55 (t, J = 6.6 Hz, 4H), 3.85 (t, J

= 5.6 Hz, 4H), 2.35 – 2.28 (m, 4H). ^{13}C NMR (101 MHz, $CDCl_3$) δ 142.60, 142.27, 134.05, 134.05, 127.41, 124.91, 120.73, 118.25, 110.77, 79.36, 79.04, 78.72, 47.52, 33.48, 31.96, 31.74. HRMS calcd for: $C_{36}H_{32}N_2O_2^+$ $[M+H]^+$: 525.2464, found: 525.2455.

1.4 Synthesis of 9,9'-(((2,5-di-tert-butyl-1,4-phenylene)bis(oxy))bis(propane -3,1-diyl))bis(9H-carbazole) (TBCP):

In a round bottom flask, 2,5-di-tert-butylbenzene-1,4-diol (111 mg, 0.5 mmol) was dissolved in 6 ml of DMF, then 9-(3-bromopropyl)-9H-carbazole (0.67 g, 2.3 mmol) and potassium carbonate (281.2 mg, 2.0 mmol) were added. And the reaction mixture was stirred under argon at 40 ℃ overnight. And then extracted with ethyl acetate (3×60 mL). The organic layer was dried over anhydrous Na_2SO_4. After removal of the solvent, the residue was purified on large silica gel plates with petroleum ether-dichloromethane (10:1) as eluent to afford the product as a white powder (10 mg, 6%). ^{1}H NMR (400 MHz, $CDCl_3$) δ 8.12 (d, J = 7.7 Hz, 4H), 7.47 – 7.42 (m, 8H), 7.25 – 7.22 (m, 4H), 6.71 (s, 2H), 4.61 (t, J = 7.0 Hz, 4H), 4.02 (t, J = 5.6 Hz, 4H), 2.38 (dt, J = 12.7, 6.3 Hz, 4H), 1.42 (s, 18H). ^{13}C NMR (101 MHz, CDCl3) δ 140.69, 137.00, 132.47, 125.53, 120.02, 118.50, 111.23, 108.76, 77.36, 77.04, 76.73, 63.81, 59.27, 54.73, 34.91, 31.63, 31.47, 29.74.. HRMS calcd for: $C_{44}H_{48}N_2O_2^+$ $[M]^+$: 636.3716, found: 636.3630.

1.5 Synthesis of 9,9'-(((2,5-dibromo-1,4-phenylene)bis(oxy))bis(propane -3,1-diyl))bis(9H-carbazole) (BBCP):

In a round bottom flask, 2,5-dibromobenzene-1,4-diol (134 mg, 0.5 mmol) was dissolved in 6 ml of DMF, then 9-(3-bromopropyl)-9H-carbazole (0.67 g, 2.3 mmol) and potassium carbonate (281.2 mg, 2.0 mmol) were added. And the reaction mixture was stirred under argon at 40 ℃ overnight. And then extracted with ethyl acetate (3×60 mL). The organic layer was dried over anhydrous Na2SO4. After removal of the solvent, the residue was purified on large silica gel plates with petroleum ether-dichloromethane (10:1) as eluent to afford the product as a white powder (20 mg, 12%). ^{1}H NMR (400 MHz, $CDCl_3$) δ 8.10 (d, J = 7.8 Hz, 4H), 7.49 – 7.44 (m, 6H), 7.41 (d, J = 8.1 Hz, 4H), 7.23 (d, J = 6.0 Hz, 4H), 4.44 (t, J = 6.9 Hz, 4H), 4.13 (t, J = 6.0 Hz, 4H), 2.22 (dd, J = 10.4, 5.0 Hz, 4H). ^{13}C NMR (101 MHz, $CDCl_3$) δ 149.78, 140.04, 125.52, 122.73, 120.34, 118.81, 112.96, 108.21, 77.36, 77.04, 76.92, 76.73, 62.81, 56.63, 29.81. HRMS calcd for: $C_{36}H_{30}Br_2N_2O_2^+$ $[M+H]^+$: 681.0674, found: 681.0731.

1.6 Sensing studies:

For solution-phase detection, an ethanol solution of explosives molecules or an aqueous solution of metal ions was incrementally added to the DMF solution of TPAK, and the fluorescence spectra were obtained accordingly. The specific types of metal salts are as follows: $Fe_2(SO_4)_3$; $CuSO_4$; $Al_2(SO_4)_3$; $Co(CH_3COO)_2$; $ZnCl_2$; $CaCl_2$; $NiCl_2$; $MgSO_4$; $SnCl_2$; $In(NO_3)_3$; $Zr(NO_3)_2$; $Mn(CH_3COO)_2$; $Eu(NO_3)_3$; $AgNO_3$; NaCl; KCl.

2. Characterization

NMR spectra were recorded with a 400-MHz spectrometer for ^{1}H NMR and a 101-MHz instrument for ^{13}C NMR using TMS as an internal standard. Chemical shifts (δ) are reported relative to TMS (^{1}H NMR), $CDCl_3$ or DMSO-d6 (^{13}C NMR). Multiplicities are reported as follows: singlet (s), doublet (d), triplet (t), quartet (q) and multiplet (m). High resolution mass spectroscopy (HRMS) was carried out using the liquid chromatography-high resolution quadrupole time-of-flight tandem mass spectrometer (Bruker microTOF-Q11-MS; APCI $[M+H]^+$) to analyze reaction products (TPAK, BCP, BBCP). High resolution mass spectroscopy (HRMS) of DCP product was carried out using Bruker solanX 70 FT-MS mass spectrometer (Bruker solanX 70 FT-MS; ESI $[M]^+$). High resolution mass spectroscopy (HRMS) of TBCP product was carried out using the Autoflex_MAX time-of-flight mass spectrometer (Autoflex_MAX MALDI TOF-MS; HESI $[M]^+$). SEM images were taken using a Hitachi SEM SU8010 field emission scanning electron microscope (FESEM). The UV-visible absorption spectrum was carried out at room temperature using a SHZMADZU UV-3600 Plus spectrophotometer. The fluorescence spectroscopy was carried out using an F-7000 fluorescence spectrometer. The fluorescence quantum yield was measured by FLS1000 fluorescence spectrometer. Deposition Numbers 2189521 (for TPAK (Block)), 2189522 (for BCP), 2189523 (for TBCP), 2189515 (for TPAK (Bar)), 2189524 (for DCP) contain the supplementary crystallographic data for this paper. These data are provided free of charge by the joint Cambridge Crystallographic Data Centre and Fachinformationszentrum Karlsruhe Access Structures service. The electrochemical properties of TPAK were investigated by cyclic voltammograms (CVs) to determine the HOMO and LUMO energy levels. The measurement was carried out in CH_2Cl_2 using carbon electrode as working electrode, Ag/AgCl as the reference electrode and Pt wire as the counter electrode. According to the CV of Figure S28b, TPAK showed irreversible oxidation behavior and the oxidation peaks appear at 0.75 eV. The HOMO energy levels can be calculated from the onset oxidation potential with reference to ferrocene (4.8 eV) by the following equation：

HOMO(eV)=-[$E_{ox(onset)vsAg/AgCl}$+4.8-E_{FOC}], whereas the LUMO energy levels can be determined based on the HOMO and the optical bandgap. The HOMO and LUMO values were determined to be -5.20 eV and -2.52 eV for TPAK.

3. Additional information

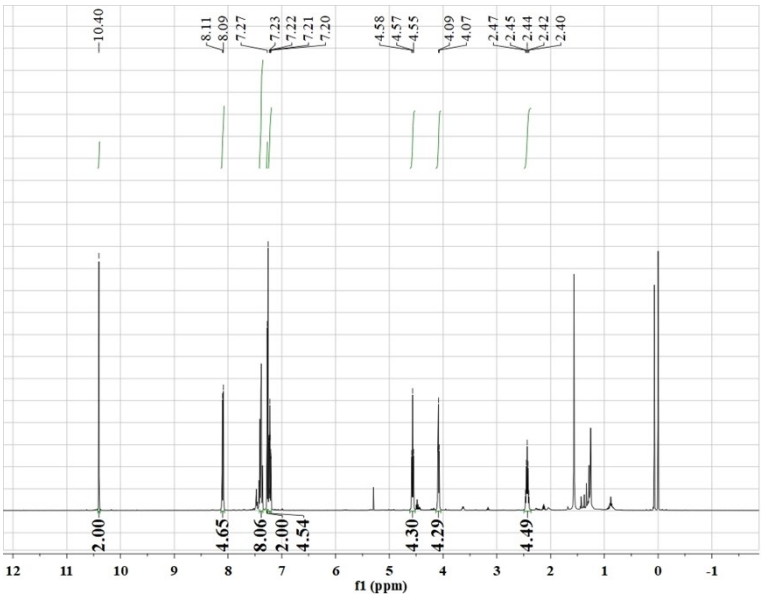

Figure S2. ^{1}H NMR spectrum of 2,5-bis(3-(9H-carbazol-9-yl)propoxy)terephthalaldehyde (TPAK) in $CDCl_3$.

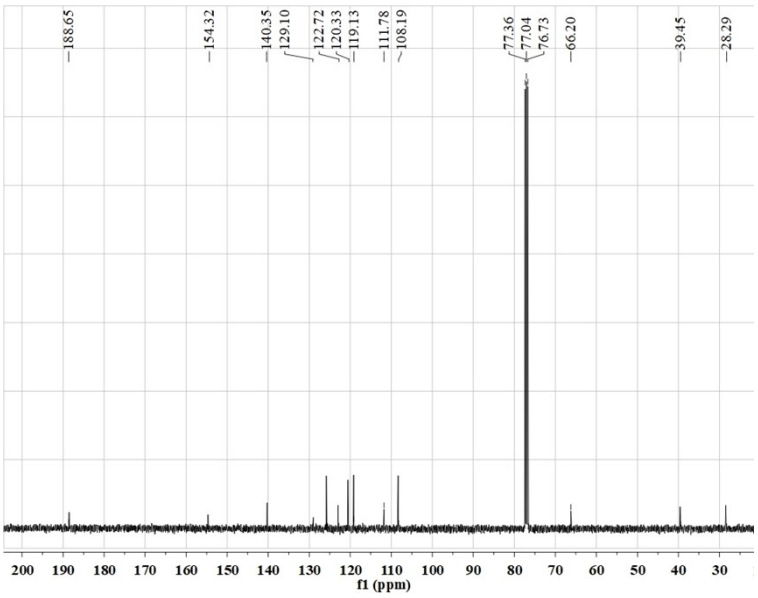

Figure S3. ^{13}C NMR spectrum of 2,5-bis(3-(9H-carbazol-9-yl)propoxy)terephthalaldehyde (TPAK) in $CDCl_3$.

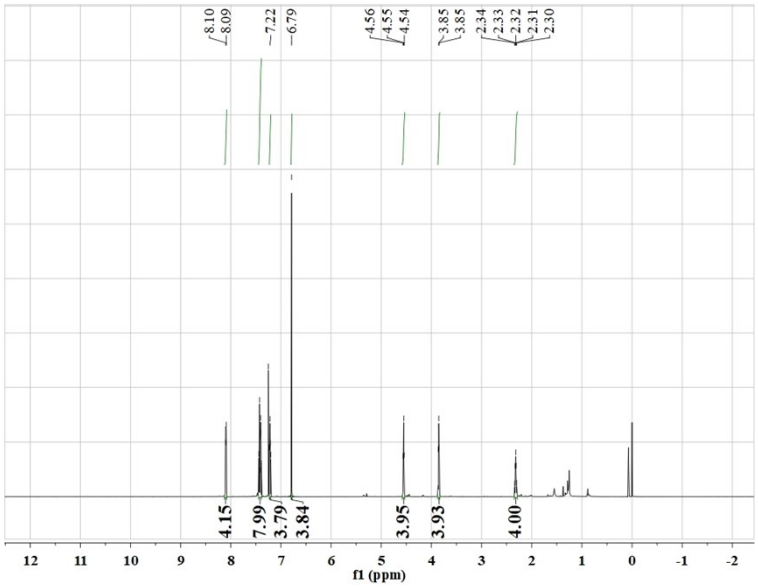

Figure S4. ^{1}H NMR spectrum of 1,4-bis(3-(9H-carbazol-9-yl)propoxy)benzene (BCP) in $CDCl_3$.

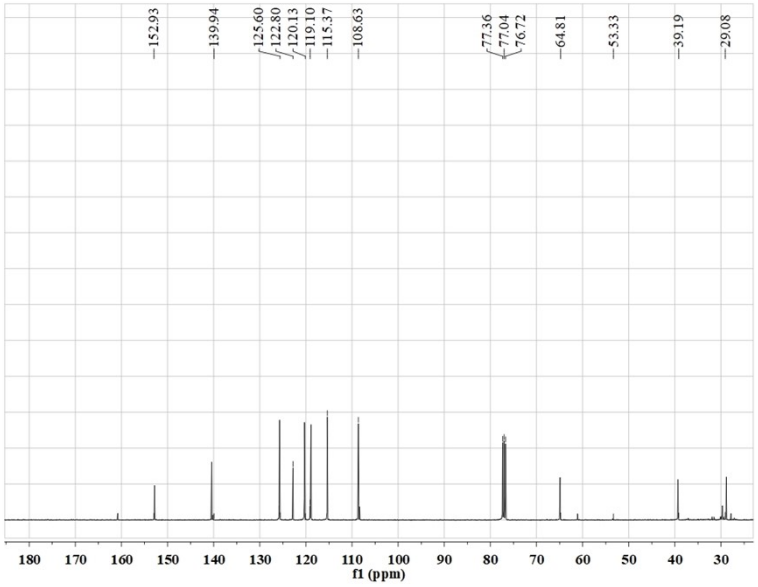

Figure S5. ^{13}C NMR spectrum of 1,4-bis(3-(9H-carbazol-9-yl)propoxy)benzene (BCP) in $CDCl_3$.

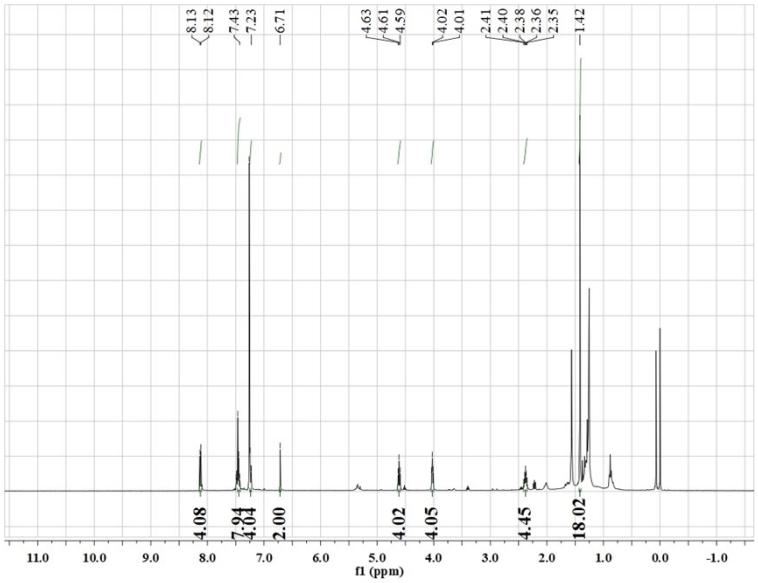

Figure S6. ^{1}H NMR spectrum of 9,9'-(((2,5-di-tert-butyl-1,4-phenylene)bis(oxy))bis(propane-3,1-diyl))bis(9H-carbazole) (TBCP) in $CDCl_3$.

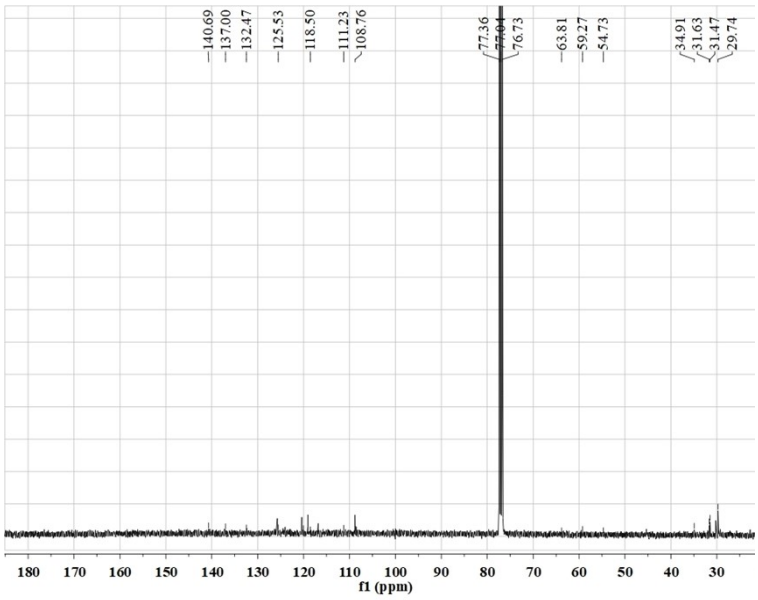

Figure S7. ^{13}C NMR spectrum of 9,9'-(((2,5-di-tert-butyl-1,4-phenylene)bis(oxy))bis(propane-3,1-diyl))bis(9H-carbazole) (TBCP) in $CDCl_3$.

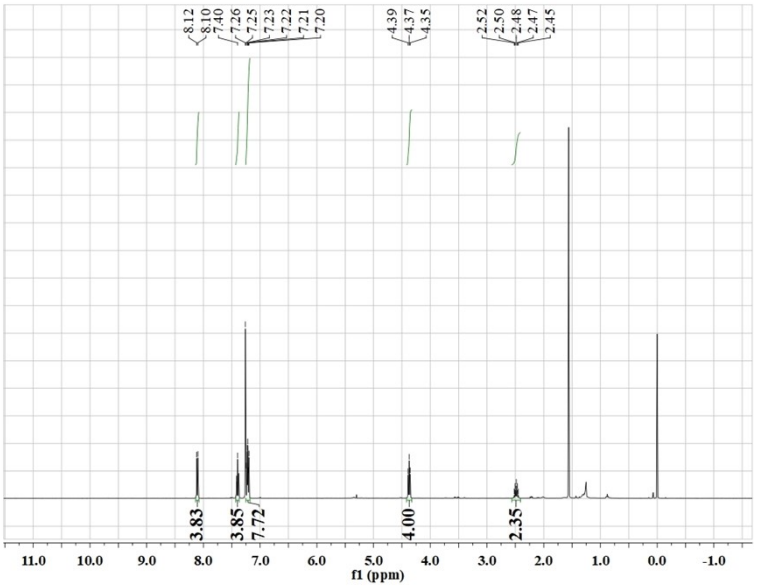

Figure S8. ^{1}H NMR spectrum of 1,3-di(9H-carbazol-9-yl)propane (DCP) in $CDCl_3$.

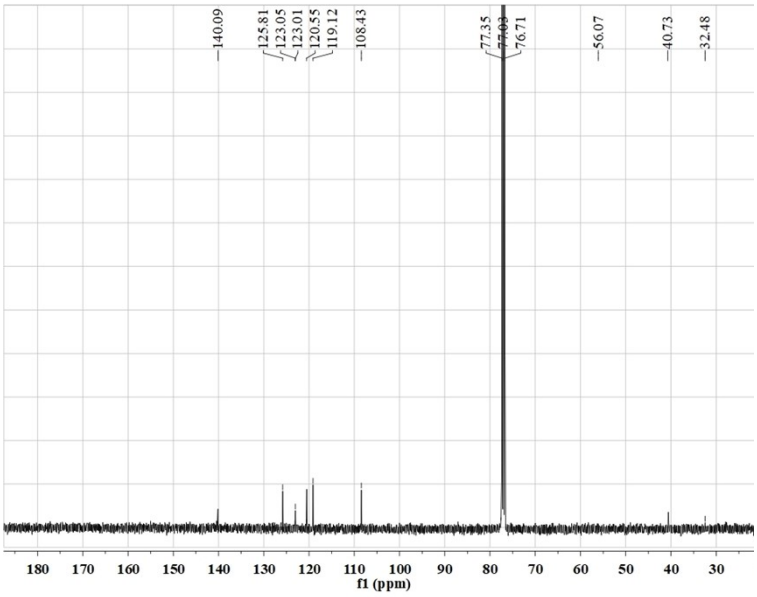

Figure S9. ^{13}C NMR spectrum of 1,3-di(9H-carbazol-9-yl)propane (DCP) in $CDCl_3$.

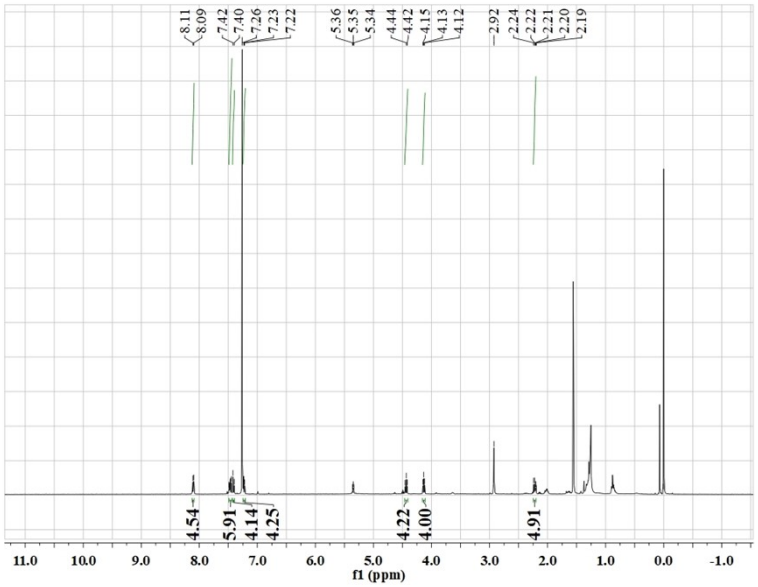

Figure S10. ^{1}H NMR spectrum of 9,9'-(((2,5-dibromo-1,4-phenylene)bis(oxy))bis(propane-3,1-diyl))bis(9H-carbazole) (BBCP) in $CDCl_3$.

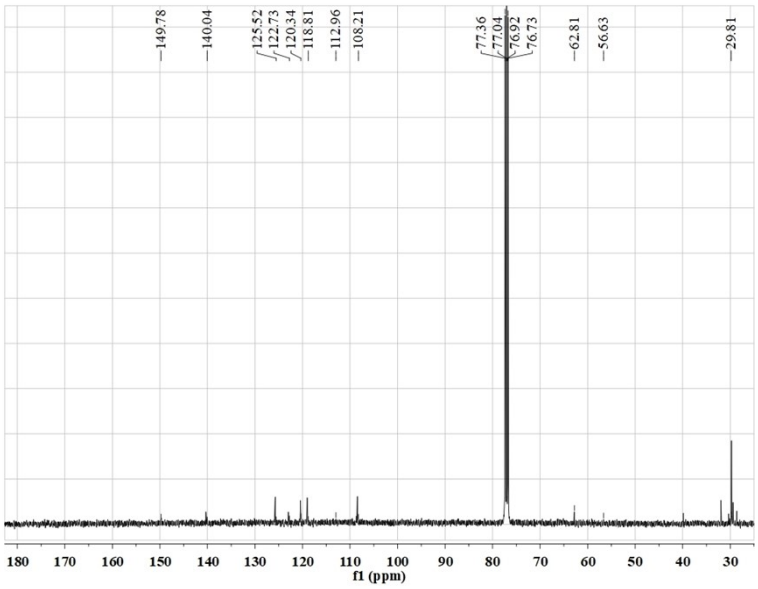

Figure S11. ^{13}C NMR spectrum of 9,9'-(((2,5-dibromo-1,4-phenylene)bis(oxy))bis(propane-3,1-diyl))bis(9H-carbazole) (BBCP) in $CDCl_3$.

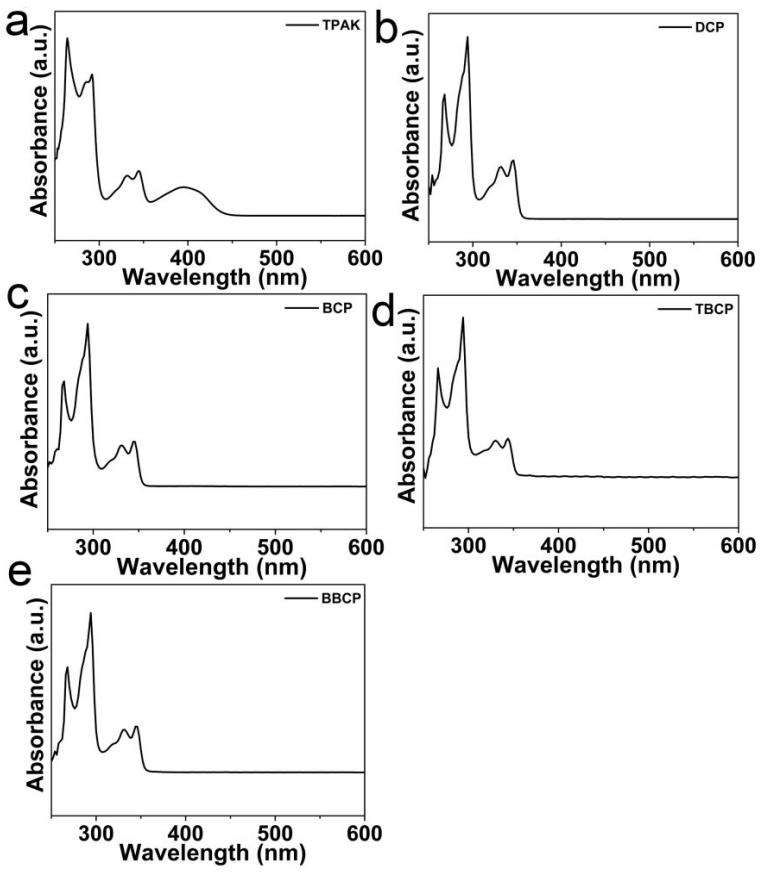

Figure S12. The UV-vis spectra of a series of biscarbazole organic small molecules (TPAK, DCP, BCP, TBCP and BBCP) in DMF solution.

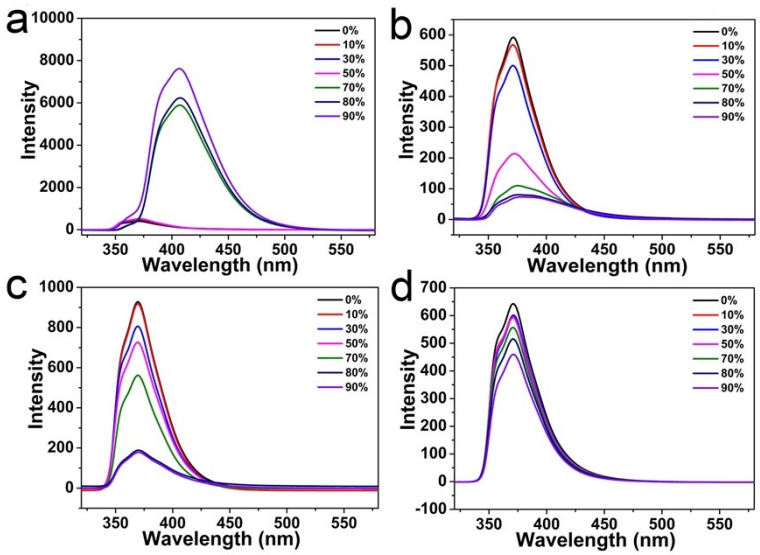

Figure S13. The fluorescence emission spectra of a series of biscarbazole organic small molecules (DCP, BCP, TBCP and BBCP) in DMF/H_2O mixtures with different water fractions (f_w).

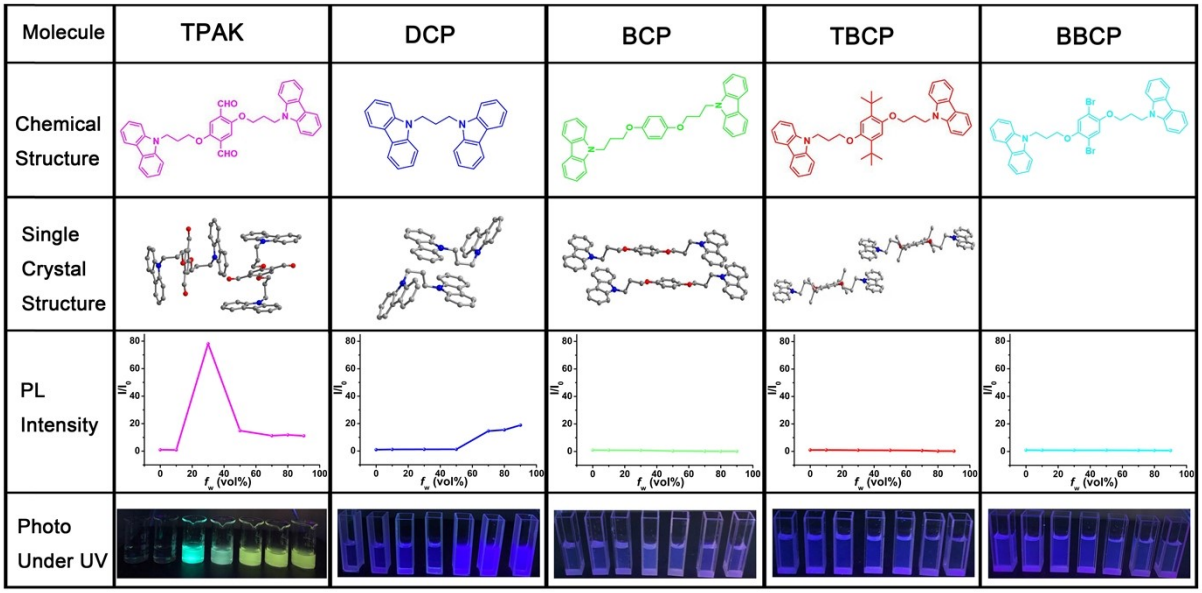

Figure S14. The molecular structures, X-ray crystallographic structures, AIE behaviors and photographs under UV light (365 nm) of a series of biscarbazole organic small molecules (TPAK, DCP, BCP, TBCP and BBCP) (Red: Oxygen atom, Blue: Nitrogen atom, Gray: Carbon atom; TPAK (λ_{ex} = 365 nm), DCP (λ_{ex} = 300 nm), BCP (λ_{ex} = 300 nm), TBCP (λ_{ex} = 300 nm) and BBCP (λ_{ex} = 300 nm); From left to right: f_w: 0%, 10%, 30%, 50%, 70%, 80%, 90%).

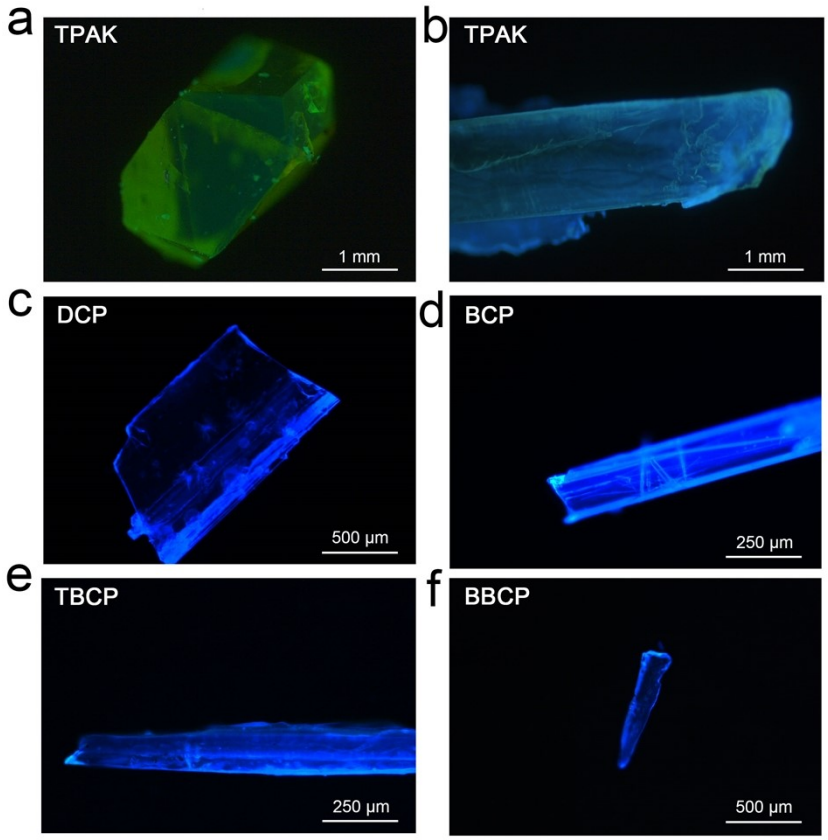

Figure S15. Fluorescence microscope photographs of a series of biscarbazole organic small molecules single crystals (TPAK (Block), TPAK (Bar), DCP, BCP, TBCP and BBCP).

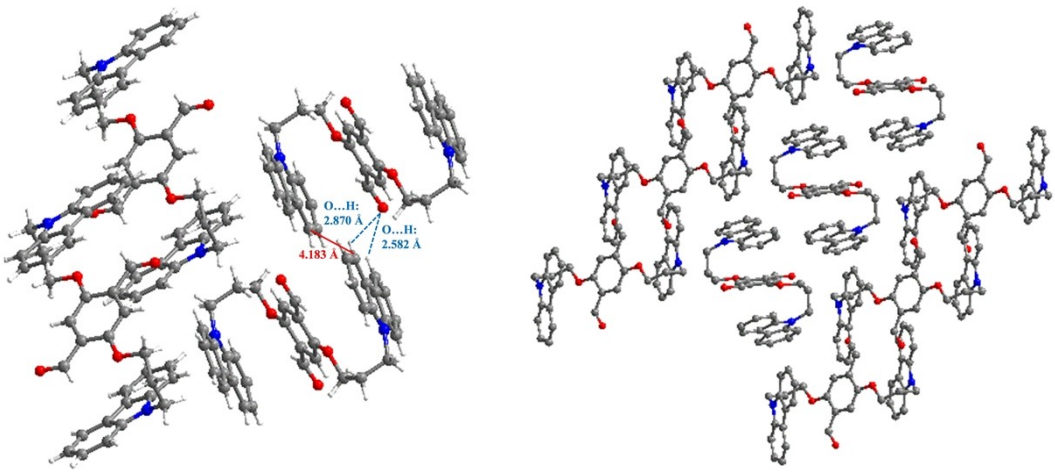

Figure S16. Stacking modes and intermolecular contacts existing in TPAK (Block) organic small molecules as identified from the X-ray crystallographic data and the contacts distances and hydrogen bonds are highlighted (Red: Oxygen atom, Blue: Nitrogen atom, Gray: Carbon atom, White: Hydrogen atom.).

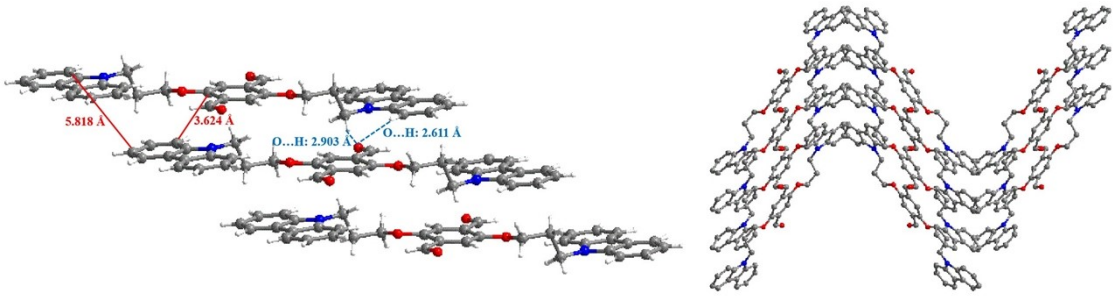

Figure S17. X-ray crystallographic structure of TPAK (Bar) as identified from the X-ray crystallographic data and Stacking modes and intermolecular contacts existing in TPAK (Bar) as identified from the X-ray crystallographic data and the contacts distances and hydrogen bonds are highlighted (Red: Oxygen atom, Blue: Nitrogen atom, Gray: Carbon atom, White: Hydrogen atom.).

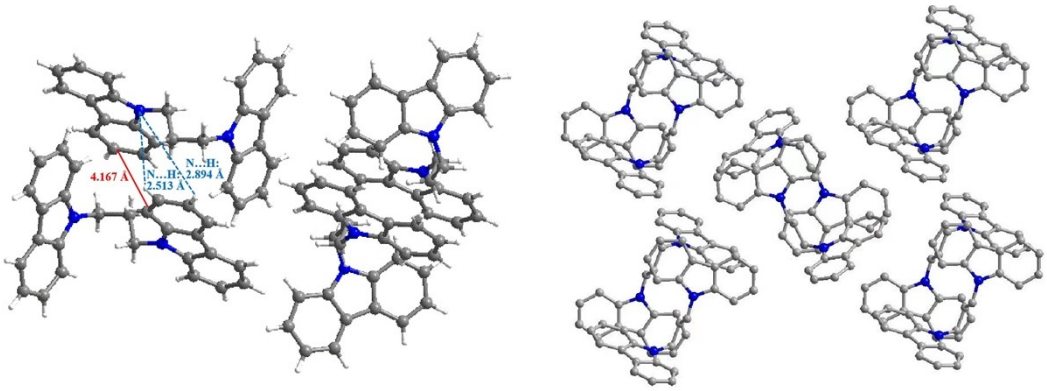

Figure S18. Stacking modes and intermolecular contacts existing in DCP organic small molecules as identified from the X-ray crystallographic data and the contacts distances are highlighted (Red: Oxygen atom, Blue: Nitrogen atom, Gray: Carbon atom, White: Hydrogen atom.).

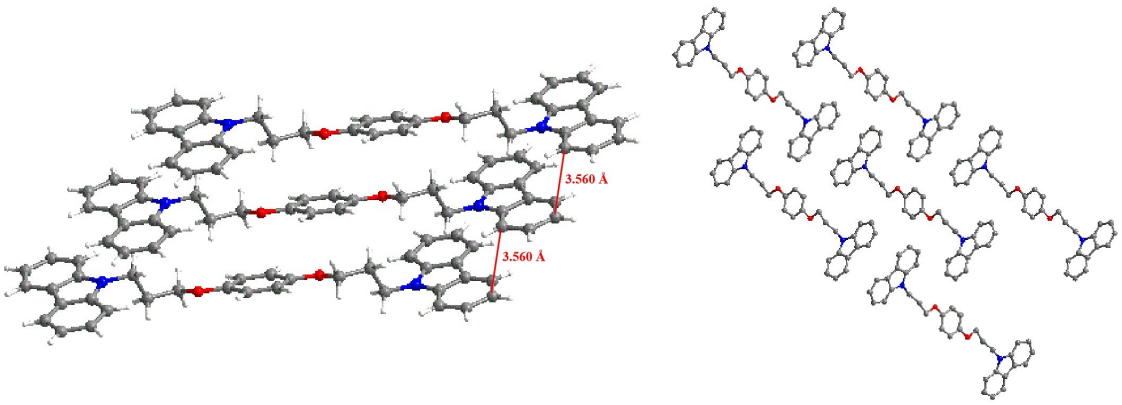

Figure S19. Stacking modes and intermolecular contacts existing in BCP organic small molecules as identified from the X-ray crystallographic data and the contacts distances are highlighted (Red: Oxygen atom, Blue: Nitrogen atom, Gray: Carbon atom, White: Hydrogen atom.).

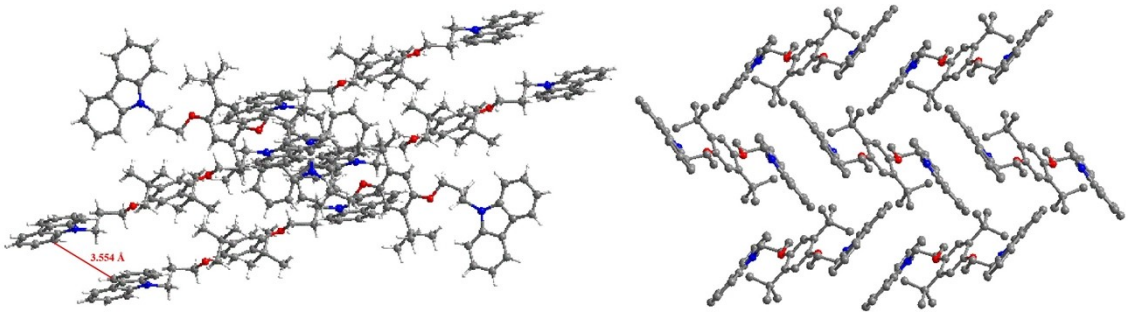

Figure S20. Stacking modes and intermolecular contacts existing in TBCP organic small molecules as identified from the X-ray crystallographic data and the contacts distances are highlighted (Red: Oxygen atom, Blue: Nitrogen atom, Gray: Carbon atom, White: Hydrogen atom.).

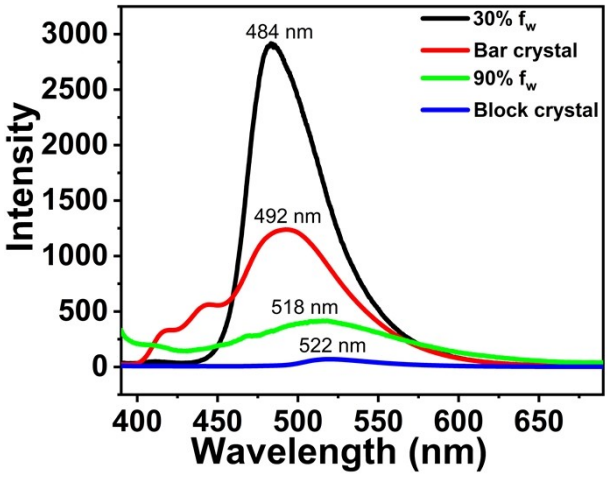

Figure S21. The fluorescence emission spectra of TPAK in DMF/H_2O mixtures with different f_w (30%, 90%) of H_2O and TPAK single crystals with different stacking mode (bar, block).

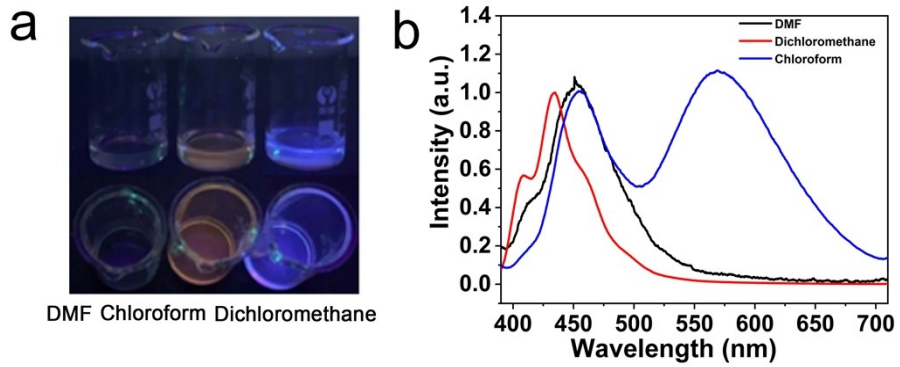

Figure S22. a. Photograph of TPAK in different solvents (DMF; Chloroform; Dichloromethane) under UV light (365 nm). **b.** Normalized fluorescence emission spectra of TPAK (λ_{ex}=365 nm) in different solvents (DMF; Chloroform; Dichloromethane). All monomer concentrations are 10^{-4} M.

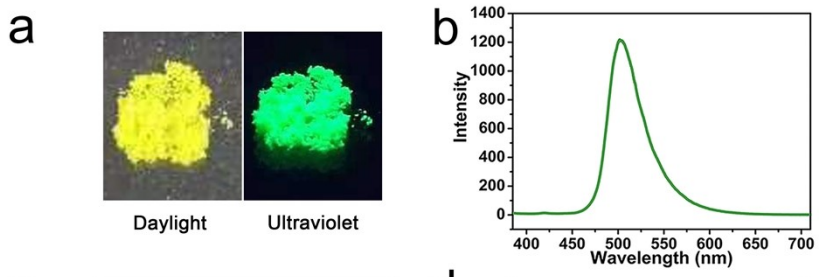

g

Percentage of H_2O	0%	10%	30%	50%	70%	80%	90%
Fluorescence quantum yield	0.01%	0.02%	2.26%	2.19%	2.15%	1.42%	1.25%

Figure S23. a. The appearance of TPAK powder under 365 nm ultraviolet (right) and daylight (left). **b.** Fluorescence emission spectrum of TPAK powder (λ_{ex} = 365 nm). **c.** TGA data of TPAK powder. **d.** XRD data of TPAK powder. **e.** OM image of TPAK powder. **f.** SEM image of TPAK powder. **g.** The fluorescence quantum yield of TPAK in DMF and H_2O mixed solution under different fractions of H_2O.

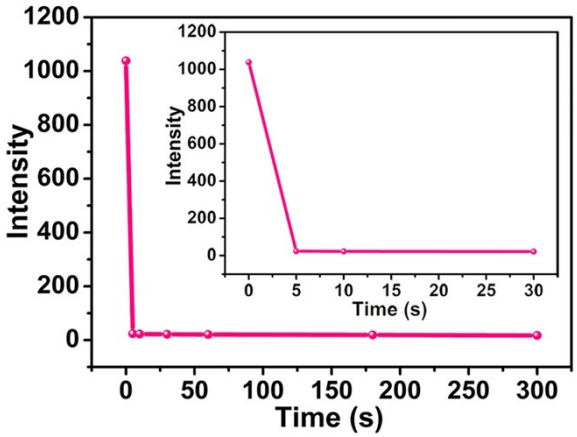

Figure S24. Fluorescence intensity at different time after adding 8.0×10^{-4} M DNP to the DMF solution of TPAK (10^{-4} M).

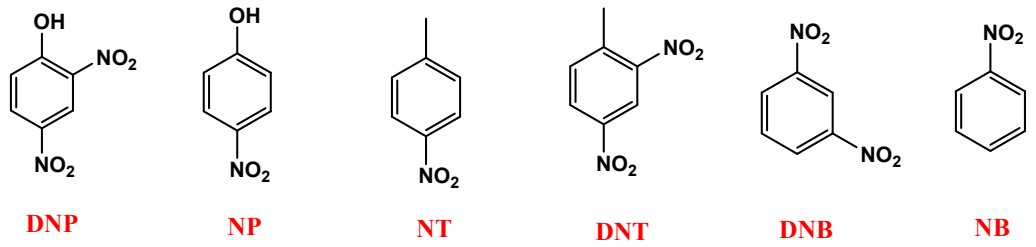

Figure S25. The molecular structures of nitroaromatics including 2,4-dinitrophenol (DNP) p-nitrophenol (NP), 4-nitrotoluene (NT), 2,4-dinitrotoluene (DNT), m-dinitrobenzene (DNB) and nitrobenzene (NB).

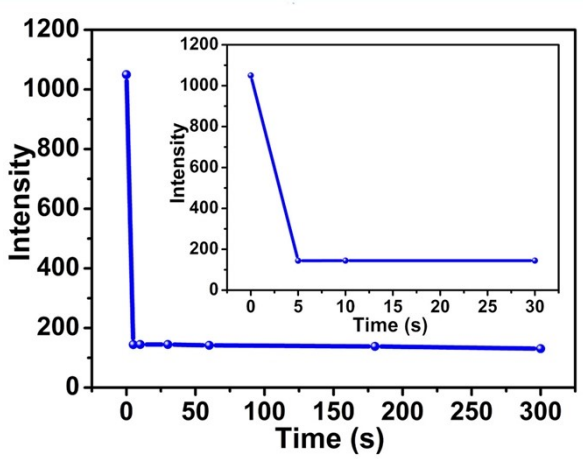

Figure S26. Fluorescence intensity at different time after adding 8.0×10^{-4} M Fe^{3+} to the DMF solution of TPAK (10^{-4} M).

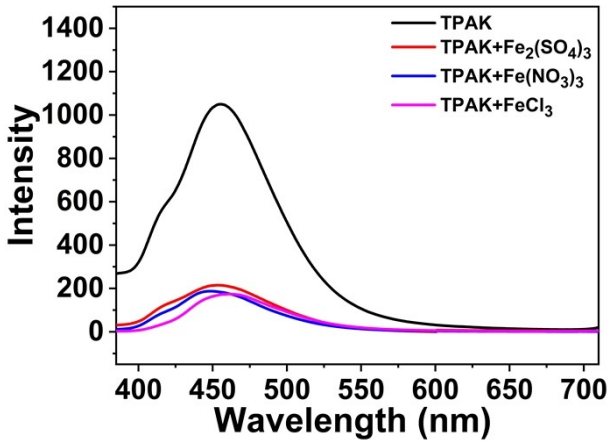

Figure S27. Fluorescence emission spectra of TPAK in DMF solution upon addition of different Fe^{3+} salts, [TPAK] = 10^{-4} M; [Fe^{3+}] = 4.0×10^{-4} M.

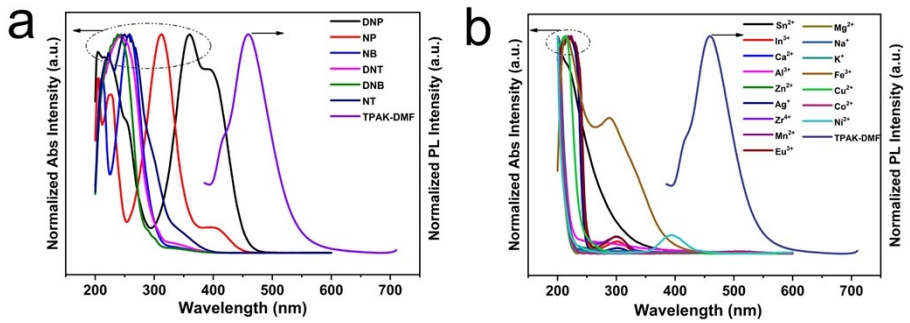

Figure S28. a. Normalized UV-vis absorption spectra of various nitroaromatics compounds in test and normalized fluorescence emission spectrum of TPAK solution. **b.** Normalized UV-vis absorption spectra of various metal ions in test and normalized fluorescence emission spectrum of TPAK solution.

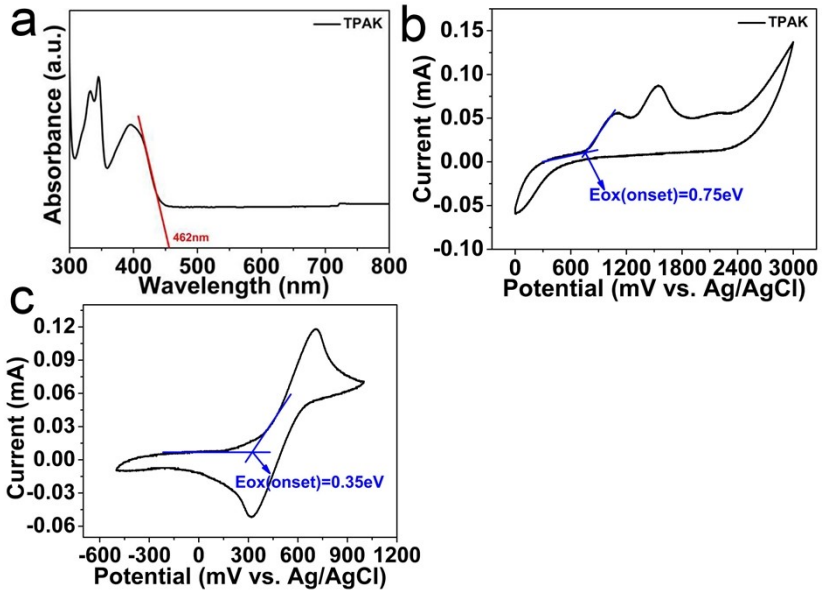

Figure S29. a. UV-vis spectrum of TPAK in DMF solution. **b.** CV curve of TPAK in 0.1 M tetrabutylammonium hexafluorophosphate (n-Bu_4NPF_6)/CH_2Cl_2 solution with platinum carbon electrode as working electrode, Ag/AgCl as the reference electrode and Pt wire as the counter electrode. **c.** The CV curve of the ferrocene standard, swept in the same conditions as for the TPAK. E_{FOC} was measured to be 0.35 eV vs. Ag/AgCl in CH_2Cl_2. The concentration of ferrocene and TPAK in CH_2Cl_2 is 0.0054 M and 0.00069 M, respectively. $E_g=h\nu=hc/\lambda=1240/\lambda=1240/462=2.68$ eV; $E_{HOMO}=-[E_{ox(onset)vsAg/AgCl}+4.8-E_{FOC}]$ =-(0.75+4.8-0.35) eV = -5.20 eV; $E_{LUMO}= E_{HOMO}+E_g$=-5.20+2.68 = -2.52 eV.

Table S1. Results for the determination of Fe^{3+} in Haihe River by the standard addition method. All concentrations were expressed as mean of three measurements.

Sample	Added (μM)	Found (μM)	Recovery (%)	RSD (%)
1	400	388.001	97.00	1.06
2	300	314.354	104.78	0.74
3	200	207.219	103.61	0.31

Table S2. Results for the determination of DNP in Haihe River by the standard addition method. All concentrations were expressed as mean of three measurements.

Sample	Added (μM)	Found (μM)	Recovery (%)	RSD (%)
1	900	880.144	97.79	4.13
2	500	536.679	107.34	5.76
3	300	277.831	92.61	3.50

Table S3. The performance of TPAK and other AIE molecules in the detection experiment of explosives.

Molecule	AIE mechanism	Nitroaromatic Explosives	Responding speed	K_{SV} (M^{-1})	LOD (M)	Linear detection range	Recovery rate	Literature
L1/L2	RIR	TNP	24 h	1.57×10^{3}	3.06×10^{-9}	0-50 μM	-	2
AIE-gens	RIR	TNP (PA)	10 min	3.33×10^{5}	3.90×10^{-8}	0-20 μM	-	3
Phosphoie oxidel	RIR	TNT	-	3.90×10^{3}	1.00×10^{-6}	0-400 μM	-	4
A_2HPS	RIR	TNP (PA)	-	1.67×10^{5}	7.20×10^{-6}	0-20 μM	-	5
PAP	RIR	TNP	-	4.70×10^{5}	1.60×10^{-9}	0-10 μM	-	6
TPAK	non-compact packed and inter-molecular hydrogen bonds	DNP	5 s	2.14×10^{4}	2.23×10^{-6}	0-3600 μM	92.61-107.34%	This work

Table S4. The performance of TPAK and other AIE molecules in the detection experiment of metal ion.

Molecule	AIE mechanism	Metal ion	Responding speed	K_{SV} (M^{-1})	LOD (M)	Linear detection range	Recovery rate	Literature
AIE-L	RIR	Zn^{2+}	5 s	1.47×10^{5}	1.10×10^{-7}	0-60 μM	-	7
TPEN	RIR	Ag^{+}	-	1.04×10^{6}	2.50×10^{-7}	0-50 μM	-	8
TPE-S	RIR	Hg^{2+}	-	2.60×10^{4}	1.00×10^{-7}	0-200 μM	-	9
p/m-TPE-RNS	RIR	Hg^{2+}	30 min	9.00×10^{7}	3.80×10^{-9}	0-25 μM	-	10
TPEThRB	RIR	Fe^{3+}	-	8.16×10^{4}	3.2×10^{-6}	0-120 μM	-	11
S1/S2	RIR	Fe^{3+}	-	1.05×10^{6} and 1.40×10^{6}	4.51×10^{-5} and 3.37×10^{-6}	0-25 μM and 0-60 μM	-	12
L1/L2	RIR	Fe^{3+}	-	1.93×10^{4}a nd 6.93×10^{4}	1.63×10^{-7} and 3.99×10^{-6}	0-40 μM and 0-25 μM	-	13
Py-BTZ	RIR	Fe^{3+}	5 min	2.59×10^{4}	2.61×10^{-6}	0-20 μM	-	14
Np-3Py/Np-4Py	RIR	Fe^{3+}	5 min	6.64×10^{6} and 1.82×10^{6}	1.07×10^{-8} and 1.02×10^{-8}	0-250 μM and 0-200 μM	-	15
TPAK	non-compact packed and inter-molecular hydrogen bonds	Fe^{3+}	5 s	2.03×10^{4}	2.31×10^{-6}	0-3600 μM	97.00-104.78%	This work

8.

9.

4. References

[1] Y. R. Song, G. Y. Feng, L. L. Wu, E. B. Zhang, C. F. Sun, D. J. Fa, Q. Liang, S. B. Lei, X. Yu, W. P. Hu, *J. Mater. Chem. C*., **2022**, 10, 2631-2638.

[2] V. P. Jejurkar, G. Yashwantrao, B. P. K. Reddy, *Chem. Photo. Chem*., **2020**, 5, 1-9.

[3] M. Z. K. Baig, P. K. Sahu, M. S. Orcid, M. C. Orcid, *J. Org. Chem*., **2017**, 82, 13359-13367.

[4] K. Shiraishi, T. Sanji, M. Tanaka, *ACS Appl. Mater. Inter*., **2009**, 1(7), 1379-1382.

[5] Y. Q. Dong, J. W.Y. Lam, A. J. Qin, Z. Li, J. Z. Liu, J. Z. Sun, Y. P. Dong, B. Z. Tang, *Chem. Phys. Lett*., **2007**, 446, 124-127.

[6] M. Shyamal, S. Maity, P. Mazumdar, G. P. Sahoo, R. Maity, A. Misra, *J Photoch Photobio A*., **2017**, 342, 1-14.

[7] M. Gao, B. Z. Tang, *ACS Sen*., **2016**, 1, 739-747.

[8] S. Umar, A. K. Jha, D. Purohit, A. G. Orcid, *J. Org. Chem*., **2017**, 82, 4766-4773.

[9] Z. J. Ruan, C. G. Li, J. R. Li, J. G. Qin, Z. Li, *Sci. Rep*., **2015**, 5, 15987-15996.

[10] Y. C. Chen, W. J. Zhang, Y. J. Cai, R. T. K. Kwok, Y. B. Hu, J. W. Y. Lam, X. G. Gu, Z. K. He, Z. Zhao, X. Y. Zheng, B. Chen, C. Gui, B. Z. Tang, *Chem. Sci*., **2017**, 8, 2047-2055.

[11] H. X. Yu, J. Zhi, Z. F. Chang, T. Shen, W. L. Ding, X. Zhang, J. L. Wang, *Mater. Chem. Front*., **2019**, 3, 151-160.

[12] C. Pan, K. Wang, S. Ji, H. Wang, Z. Li, H. He, Y. Huo, *RSC Adv*., **2017**, 7, 36007-36014.

[13] J. Harathi, K. Thenmozhi, *Mater. Chem. Front*., **2020**, 4, 1471-1482.

[14] S. D. Padghan, A. L. Puyad, R. S. Bhosale, S. V. Bhosale, S. V. Bhosale, *Photochem. Photobiol. Sci*., **2017**, 16, 1591-1595.

[15] A. Mukherjee, M. Chakravarty, *New J. Chem*., **2020**, 44, 6173-6181.